On the Role of Different Adsorption and Reaction Sites on Supported Nanoparticles during a Catalytic Reaction: NO Decomposition on a Pd/Alumina Model Catalyst†

V. Johánek,‡ S. Schauermann,‡ M. Laurin,‡ Chinnakonda S. Gopinath,§ J. Libuda,*,‡ and H.-J. Freund‡

Fritz-Haber-Institut der Max-Planck-Gesellschaft, Department of Chemical Physics, Faradayweg 4-6, 14195 Berlin, Germany, and National Chemical Laboratory, Catalysis Division, Pune 411 008, India

Received: December 31, 2003; In Final Form: April 1, 2004

We have studied the catalytic decomposition of NO on a structurally well-defined Pd model catalyst, employing a combination of molecular beam techniques and time-resolved IR reflection absorption spectroscopy (TR-IRAS). In a first step, different active sites such as facets and edges/defects on the catalyst nanoparticles are identified spectroscopically. Subsequently, these spectroscopic signatures are utilized to monitor the site occupation by reactant species (NO) and products (atomic oxygen and nitrogen) under reaction conditions. Simultaneously, the kinetics of NO dissociation is investigated. It is found that atomic nitrogen and oxygen species are initially formed in the vicinity of edge or defect sites. At temperatures up to 300 K, the mobility of these atomic species is suppressed, whereas at higher temperature, diffusion onto the (111) facets of the particles can occur. It is shown both by IR spectroscopy of adsorbed NO under reaction conditions and by control experiments using CO as a probe molecule that nitrogen and oxygen species preferentially occupy particle edge and defect sites. By means of molecular beam CO titration experiments and TR-IRAS, it is demonstrated that the presence of these atomic species critically controls the NO dissociation activity. Specifically, the presence of strongly bound nitrogen in the vicinity of edge and defect sites gives rise to an enhanced dissociation probability under conditions of high adsorbate coverage.

1. Introduction

Most supported catalysts are composed of active particles in the nanometer size range, which typically are dispersed on a high-surface-area oxide support. At their surface, these particles expose a variety or nonequivalent adsorption and reaction sites such as particle edges, corners, steps or defects, and different crystallite facets or interface sites at the particle perimeter. In the case of sufficiently small particles or strong support interactions, the properties of these sites might be additionally modified.

It is the properties of these different reactive sites and their complex interplay that control the kinetics of catalytic reaction on the particle surface. For technical applications, the resulting structure- and size-dependent effects are often taken advantage of by empirically optimizing the structural properties of the catalyst via the parameters employed in the preparation procedure. (See, for example, ref 1.) On the microscopic level, however, the origins of such effects remain unexplained in most cases because the intrinsic complexity of the catalyst surfaces precludes a detailed understanding.

To overcome this problem, a model catalyst approach has been pursued by our group and others.[2−5] These models allow us to replicate certain structural features of a catalyst surface without having to deal with the full complexity of the real system. Here, we utilize a Pd model catalyst, which is prepared under ultrahigh-vacuum (UHV) conditions on an ordered Al_2O_3 film.[6,7] This system has been characterized in great detail with respect to its geometric and electronic structure and its adsorption properties.[8]

Recently, we have started to perform molecular beam experiments on these supported model catalysts.[9] The molecular beam approach makes available quantitative kinetic data under flexible and exceptionally well-controlled experimental conditions. In combination with the model systems, it may provide unique insights into the kinetics on complex surfaces at the microscopic level, as has recently been shown for different reaction systems.[10−12]

In this work, we focus on a key issue in reaction kinetics on heterogeneous surfaces, on which, however, there is very little information available: We study the distribution of adsorbed species under reaction conditions over the different sites available on the surface of the catalyst particles. It is shown that specific atomic adsorbates, which are often present under reaction conditions, show a strong preference for specific sites on the catalyst particles. Moreover, their presence or absence in the vicinity of these sites is shown to control the kinetics of the reaction. Thus a thorough understanding of this type of coadsorbate systems is a vital ingredient in the microscopic description of catalytic activity.

As a model reaction in this study, we investigate the dissociation and reduction of NO. Recently, the catalytic reduction of NO_x has attracted considerable attention in environmental catalysis,[13] and the use of supported Pd catalysts (see, for example, refs 14−16 and references therein) has been explored in addition to the more traditional Rh-based systems (e.g., ref 17 and references therein; also refs 18 and 19). Surface

† Part of the special issue "Gerhard Ertl Festschrift".

* Corresponding author. E-mail: libuda@fhi-berlin.mpg.de. Fax: +49-30-84134309.

‡ Fritz-Haber-Institut der Max-Planck-Gesellschaft.

§ National Chemical Laboratory.

10.1021/jp031371f CCC: $27.50
Published on Web 07/03/2004

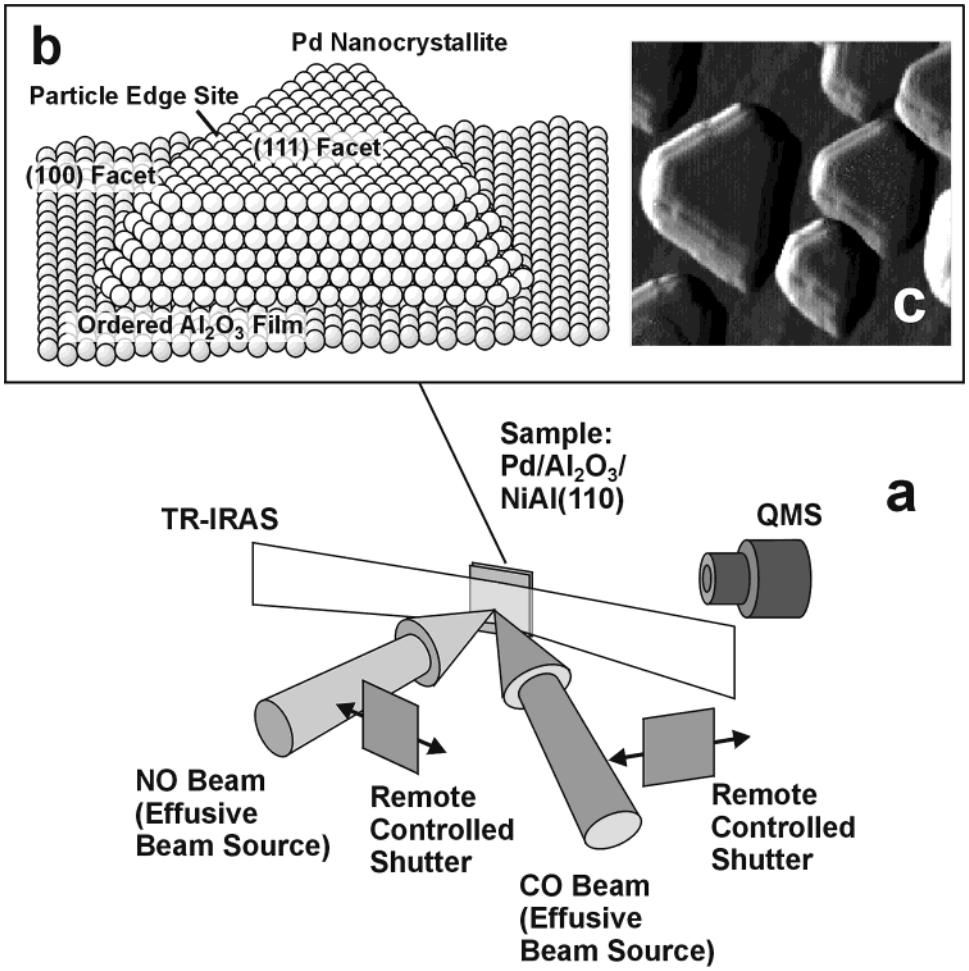

Figure 1. (a) Schematic representation of the experimental molecular beam setup used in this work; (b) schematic model of the Pd particles on the surface of the supported model catalyst; (c) STM image showing the Pd particles on Al_2O_3/NiAl(110) (20 nm × 20 nm, from ref 31).

science experiments on the origin of structure-dependent reactivity effects have been performed both on Pd single crystals[20−25] and on supported Pd model catalysts,[26,27] and it has been noted previously that the atomic dissociation products of NO may play a key role in the reaction kinetics.[24]

In the current work, we utilize multiple molecular beam methods and in-situ TR-IRAS (time-resolved IR reflection absorption spectroscopy) to investigate in detail the role of atomic nitrogen and atomic oxygen in the adsorption and dissociation of NO. As a basis for the kinetic studies presented, we have previously studied the interaction of NO with the alumina model support[28] as well as the adsorption of NO and the coadsorption with CO and oxygen on the supported Pd particles,[29] and we refer to these studies for details.

2. Experimental Section

All experiments were performed in a UHV molecular beam apparatus at the Fritz-Haber-Institute (Berlin), which allows up to three beams to be crossed on the sample surface.[30] A schematic representation of the experimental setup is given in Figure 1a. The NO beam (Messer Griesheim, 99.5%) and the CO beam (Linde, 99.997%) are generated by doubly differentially pumped effusive multichannel array sources after further purification of the gases by cold traps and filters (Mykrolis), respectively. For all experiments, the NO beam intensity was 2.8×10^{14} molecules·cm^{-2}·s^{-1}, and the CO beam intensity was 2.9×10^{14} molecules·cm^{-2}·s^{-1}. For reaction rate measurements, an automated quadrupole mass spectrometer system (ABB Extrel) was employed. IR spectra were acquired during exposure to the NO beam using a vacuum FT-IR spectrometer (Bruker IFS 66v/S) at a spectral resolution of 2 cm^{-1}, and the spectral features were quantified by integrating between the peak onset and the spectral minimum. The spectra in Figure 3 were recorded at NO exposures not exceeding 1.1×10^{16} molecules·cm^{-2}.

IR spectra of CO (Figure 7) on nitrogen and oxygen precovered samples were recorded at 100 K after CO saturation at 300 K (20 L CO; 1 L = 10^{-6} Torr·s). The nitrogen and oxygen precovered surface was prepared by exposure to NO (effusive beam, approximately 2600 L) at 440 K; subsequently, oxygen was selectively removed by exposure to CO (CO, effusive beam, 20 L) at 430 K. For the experiments involving the removal of surface oxygen by CO (Figure 8), CO pulses with a duration of approximately 30 s (beam intensity 2.9×10^{14} molecules·cm^{-2}·s^{-1}) were applied.

The alumina film was prepared by the sputtering and annealing of a NiAl(110) single crystal, followed by an oxidation and annealing procedure, the details of which are given elsewhere.[7] The cleanliness and quality of the oxide film were checked via LEED (low-energy electron diffraction) and AES (Auger electron spectroscopy). Before the experiment, Pd (>99.9%) was deposited by evaporation from a rod using a commercial evaporator (Focus, EFM 3) based on electron bombardment (Pd coverage 2.7×10^{15} cm^{-2}; sample temperature 300 K). The evaporator flux was calibrated by a quartz microbalance prior to use. To avoid damage by ion bombardment, the sample was biased during Pd evaporation. After

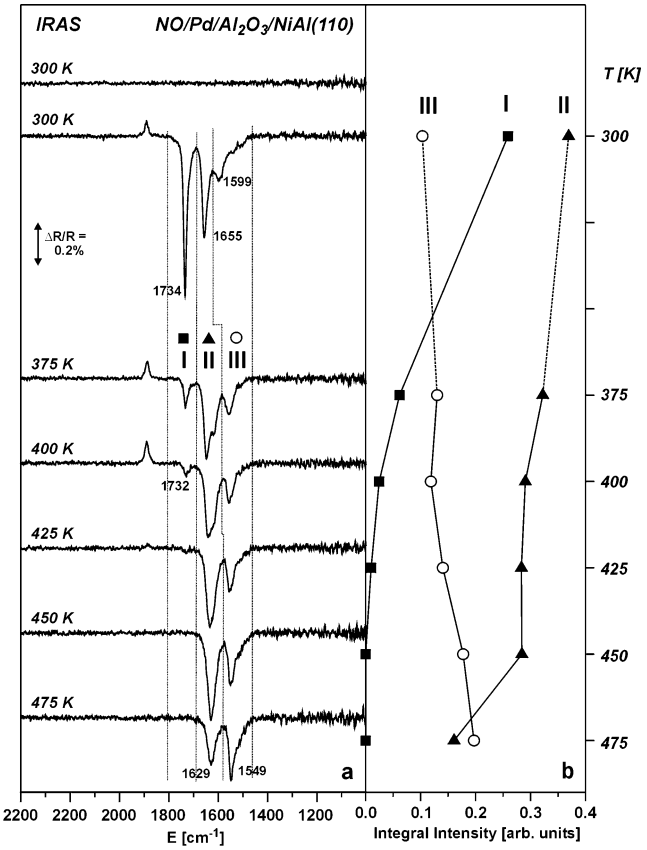

Figure 2. (a) IR spectra of the NO stretching frequency region for the Pd/alumina model catalyst recorded at various sample temperatures during NO exposure immediately after admission of the beam; (b) integral absorption in the spectral region indicated in part a.

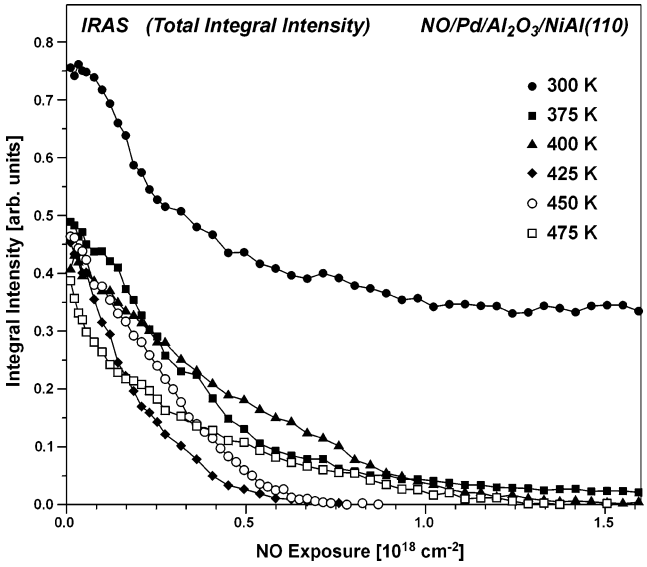

Figure 3. Total integral absorption in the NO stretching frequency region as a function of the NO dose and the surface temperature during exposure of the Pd/alumina model catalyst to a molecular beam of NO.

preparation, the Pd particles were stabilized by extended exposure to oxygen (2.7×10^{14} molecules·cm^{-2}·s^{-1}, 2400 s, sample temperature 495 K), followed by surface oxygen removal by CO and the thermal desorption of remaining CO.[31,32]

3. Results and Discussion

3.1. Structure of the Pd Model Catalyst. The structure of the Pd model catalyst particles represents one of the key prerequisites in this study. For this reason, we briefly summarize the previous results on the $Pd/Al_2O_3/NiAl(110)$ model catalyst in as far as they are relevant to the present work. For more detailed information on structure and adsorption properties, we refer to the literature.[7,8,31] A schematic representation of the Pd particles is displayed in Figure 1b. For the specific system considered in this work, the 3D Pd aggregates are characterized by a mean particle size of 5.5 nm. On average, the particles contain about 3000 atoms, 20% of which are located at the surface. The majority of particles exhibits the morphology of well-shaped crystallites, which grow in the (111) orientation and are predominantly terminated by (111) facets. Additionally, a small fraction of (100) facets is exposed. For the given preparation conditions, the particle density was $1.0(\pm 0.2) \times 10^{12}$ cm^{-2}. About 20% of the support surface is covered by Pd particles. For experiments requiring elevated temperatures, the samples were stabilized by oxygen treatment at elevated temperatures, followed by oxygen removal by CO titration and, finally, the thermal removal of remaining CO.[31,32] Note that neither the particle shape nor the density is affected by this procedure.

3.2. In-Situ IR Spectroscopy of NO Adsorption on the Pd Model Catalyst. The first step toward a site-dependent study of the NO dissociation process is the spectral assignment of the corresponding IR absorption bands under reaction conditions. For this purpose, IR spectra were acquired during the exposure of the pristine Pd model catalyst to an NO beam, immediately after switching on the beam (i.e., before an appreciable amount of NO has been dissociated).

Corresponding spectra of the NO stretching frequency region as a function of sample temperature in the range from 300 to 475 K are displayed in Figure 2a. Absorption spectra at lower sample temperature have been discussed elsewhere.[29] Three spectral regions are identified, denoted as (I) to (III). The corresponding integral intensities are shown in Figure 2b. The band in region (I) between 1734 and 1732 cm^{-1} dominates in the low-temperature limit but rapidly decreases in intensity with increasing sample temperature and finally vanishes above 400 K. The absorption in region (II) shows a more complex structure containing at least two subbands. With the sample temperature increasing up to 450 K, it decreases only slightly in intensity and simultaneously shifts from 1655 cm^{-1} at 300 K to 1629 cm^{-1} at 475 K. Finally, the absorption in region (III) is weak at low temperature (300 K) but continuously increases in intensity as the sample temperature increases and the features in regions (I) and (II) become weaker. The band extends down to approximately 1450 cm^{-1} with a maximum shifting from 1599 cm^{-1} at 300 K to 1549 cm^{-1} at 475 K.

It should be noted that no NO adsorption occurs on the alumina support under the experimental conditions applied here.[28] The small negative band at 1900 cm^{-1} is due to minor CO contamination, which is inevitable during preparation and which is displaced upon NO exposure. Thus, all positive bands are due to NO chemisorbed on the Pd particles; consequently, we may attempt to derive an assignment of these bands on the basis of experimental data available for NO adsorption on Pd single-crystal surfaces.

The largest fraction of the particle surface is terminated by (111) facets. In previous NO adsorption studies on Pd(111) single crystals, it has been found that at room temperature and above, NO typically forms a disordered adsorbate phase with coverages of up to $\theta = 0.33$.[33,34] In vibrational studies at 373 K, a single band has been observed to shift from 1540 to 1590 cm^{-1} with increasing coverage.[20,21] For NO saturation at 300

K, a single band at 1589 cm^{-1} was reported.[33,34] It is important to note that under UHV conditions higher NO coverage on Pd(111) cannot be obtained at room temperature, but at cryogenic temperatures only (cf. refs 33 and 35). Here, several ordered adsorbate structures have been identified, such as an ordered c(2 × 4) phase ($\theta = 0.50$; absorption bands around 1600−1620 cm^{-1}; see refs 33, 34, 36, and 37), a (2 × 2) structure at 100 K ($\theta = 0.75$; absorption bands at 1589−1600 and 1735−1750 cm^{-1}; see refs 20, 33, 34, and 36) and intermediate phases.[37] Recently, the local NO sites for these adsorbate structures have been investigated theoretically,[38−40] and it was concluded that NO occupies fcc hollow sites at low coverage ($\theta = 0.33$), a mixture of fcc and hcp sites at intermediate coverages ($\theta = 0.5$), and on-top sites in addition to the mixture of fcc and hcp sites in the high-coverage limit ($\theta = 0.75$). It should be noted at this point that older studies often contain misassignments of sites, as recently discussed by Brown and King.[41]

As a small fraction of the Pd model catalyst particles is terminated by (100) facets, we briefly consider NO adsorption on Pd(100) as well. At elevated temperature (420 K), a p(4 × 2) superstructure ($\theta = 0.25$) is formed, giving rise to a single absorption band at 1492 cm^{-1}.[42] At 400 K and below, a second band at 1653 cm^{-1} emerges, which shifts to higher frequency with decreasing temperature and increasing coverage ($\theta = 0.50$ at 250 K; ($2\sqrt{2} \times 2\sqrt{2}$)R45°; single absorption band at 1678 cm^{-1}). In a similar manner as for Pd(111), the site occupation was reinterpreted recently, concluding that 4-fold hollow sites are occupied in the low-coverage regime, whereas at higher coverage NO adsorbs on bridge sites.[43]

In addition to the facets, the catalyst particles expose a large fraction of irregular sites such as particle edges, corners, and steps. Although there is no single-crystal equivalent of a particle edge, a rough idea of the adsorption behavior of these sites might be gained from studies on open and stepped Pd surfaces. For NO adsorption on Pd(112) at 373 K, for example, an additional band was observed in the spectral region between 1655 and 1670 cm^{-1},[20,21] which can be associated with NO bound to the step sites. Recently, similar results were reported for NO on Pd(311).[44]

On the basis of the single-crystal data, we can assign the spectral features observed for NO adsorption on the Pd model catalyst as follows:

The band in region (III) shows good agreement with the single-crystal data for NO on Pd(111); consequently, we assign the absorption in this region to NO adsorbed at hollow sites on the (111) facets of the Pd particles. There is no clear signature of NO adsorbed on the hollow sites of the (100) facets, apart from a very weak shoulder around 1500 cm^{-1}. However, the low intensity of the (100) induced band is consistent with the low surface fraction of (100) facets. Additionally, it has to be taken into account that the (100) facets of the Pd crystallites are highly tilted with respect to the surface normal, which leads to a reduced intensity due to the metal surface selection rule (MSSR). (Note that the MSSR applies to this model catalyst because of the oxide film on the underlying metal substrate is thin.[45])

The band in region (I) can be assigned to NO adsorbed at on-top sites on the Pd particles. It is noteworthy, however, that neither on Pd(111) nor on Pd(100) on-top sites can be populated under the experimental conditions applied in our experiments. Whereas from Pd(111) on-top NO desorbs at temperatures around 250 K[33,35] and on Pd(100) no on-top species are present at the same temperature,[42] on the Pd particles on-top NO can be detected up to temperatures of 400 K. Consequently, we tentatively assign this absorption band to an NO species bound to particle-specific sites such as edges and steps. This assignment is corroborated by the observation that a second and more intense band appears at slightly higher energy for adsorption at lower sample temperature, which accordingly can be assigned to on-top NO on the (111) facets themselves. For the corresponding adsorption spectra and a detailed discussion, we refer to the literature.[29]

Finally, there are the bands in region (II) for which there is no counterpart on Pd(111) single-crystal surfaces. A part of the absorption in this region might be due to NO on the (100) facets. On the basis of the arguments given above on the intensity of the (100) bands (i.e., the small fraction and the large tilt angle of the corresponding facets) and the fact that in region (III) hardly any indication of (100) facets can be identified, we conclude that the (100) contribution to absorption in this region is minor. Instead, we assign the bands to NO adsorbed at particle edges and steps. This interpretation is fully consistent with the vibrational studies for NO on stepped surfaces discussed above.

The origin of the shoulder and splitting appearing at some temperatures in region (II) is not yet clear and might be due to the presence of nonequivalent sites at the edges and steps due to the formation of specific high-coverage adsorbate structures (e.g., coupling to neighboring on-top NO at the particle edges) or may be partially due to the presence of (100) facets. On the basis of the frequency range, we may speculate that we are dealing with a bridge-bonded NO species in this region, but detailed calculations are necessary to verify any site assignments. It is noteworthy that very similar behavior was recently found for the case of CO adsorption on the same Pd particles, where bridge-bonded CO at the particle edges gives rise to a strong absorption signal in addition to the facet induced bands.[46] CO adsorption will be discussed in more detail in section 3.4.

A summary of the band assignments is given in Table 1. As a final remark it should be noted that the relative intensities of the NO bands do not reflect the relative concentrations of the corresponding species. There are several possible reasons for this effect, including differences in the dynamic dipole moment of different modes as a function of the local adsorption geometry and the electronic coupling to the metal, a different orientation of the molecules in combination with the MSSR discussed above, and intensity transfer between neighboring bands due to dipole coupling. (See, for example, ref 47.) These effects have to be kept in mind when we discuss the time or temperature dependence of the various bands; therefore, we will mainly restrict ourselves to qualitative conclusions in the following text.

Upon inspection of the temperature dependence of the NO spectra (Figure 2b), it is evident that the defect and edge sites leading to bands in region (I) are depopulated in a temperature range between 300 and 400 K and that the edge and defect sites inducing bands in region (II) remain occupied up to 450 K. Only at higher temperatures, desorption becomes fast enough to depopulate these sites during exposure to the NO beam. The hollow sites giving rise to absorption in region (III) remain occupied over the full temperature range investigated. The increase in intensity of the corresponding bands with increasing temperature most likely does not reflect an increasing occupation of these sites but is rather a consequence of the decreasing dipole coupling to the other types of NO and the changes in electronic coupling to the Pd.

In summary, we can spectroscopically distinguish between NO species adsorbed on regular facet sites and those adsorbed

TABLE 1: Assignments of Bands in the NO and CO Stretching Frequency Region Used in This Work

system	frequency region/cm^{-1}	assignment, comments	reference
NO/Pd/Al_2O_3/NiAl(110)	1732−1734 (region I)	on-top NO at particle edges, steps, defects	this work, 29
	1750 (region I)	on-top NO on (111) facets; only at surface temperatures below 200 K	29
	1629−1655 (region II)	NO at particle edges, steps, defects; minor contribution of (100) facets	this work, 29
	1549−1599 (region III)	NO at (111) facets	this work, 29
	∼1500 (region III)	NO at (100) facets (weak)	this work, 29
CO/Pd/Al_2O_3/NiAl(110)	2087−2108	on-top CO on (111) facets	46, 58
	∼2070	on-top CO at edges, defects of steps (weak)	46, 58
	1950−2000	CO at particle edges, steps, defects; minor contribution of (100) facets	11, 46, 58, 61
	1800−1930	CO on (111) facets	46, 58

at defects sites such as particle edges and steps. The corresponding spectroscopic features can be observed at elevated sample temperatures up to approximately 475 K (i.e., over a temperature range where NO dissociation occurs). In the following text, we will utilize corresponding spectra recorded during NO dissociaton in order to derive site-specific information on the dissociation processes.

3.3. NO Dissociation Kinetics and Site Occupation. To investigate the dissociation kinetics, the pristine Pd catalyst surface is exposed to an NO beam, and IR spectra are recorded as a function of time and exposure. In Figure 3, the total integral intensity in the NO stretching frequency region as derived from this type of experiment is displayed for different sample temperatures.

The principal observation from this plot is that the band intensities in the NO stretching frequency range decrease with the exposure time. This effect can be attributed to an accumulation of the dissociation products (i.e., atomic nitrogen and oxygen), which block the NO adsorption sites. The rate at which the absorption signal decreases depends on the surface temperature, indicating that the maximum rate of nitrogen and oxygen accumulation is reached at a sample temperature around 425 K. The most interesting point with respect to the following discussion, however, is the observation that at a reaction temperature of 300 K the NO signal approaches a constant residual value of approximately 45% of the initial intensity. In contrast to this, the NO absorption capacity at reaction temperatures of 375 K and above is completely lost after prolonged NO exposure.

To obtain site-specific information on the dissociation kinetics, we analyze the spectral information contained in the corresponding IR data. A representative set of IRAS spectra of the NO stretching frequency region for a sample temperature of 375 K is displayed in Figure 4a. Immediately after exposure to the NO beam, absorption features in the three NO stretching frequency regions appear. As a function of time, all three absorption bands decrease in intensity and nearly vanish in the high-exposure limit. It is apparent, however, that the three bands exhibit an entirely different dependence on exposure. To investigate these differences, the partial integral intensities in the three regions are determined as a function of the NO dose (Figure 4b). It is found that the bands in regions (I) and (II) decrease in intensity immediately after admission of the beam, with on-top NO band (I) showing the steepest decrease as a function of exposure. In contrast, the band in region (III) remains unaffected initially (or even shows a slight increase, which, however, is not necessarily due to a larger density of the corresponding NO species but more likely due to dipole coupling or coverage-dependent electronic effects). Only at higher NO doses does the band in region (III) start to drop in intensity.

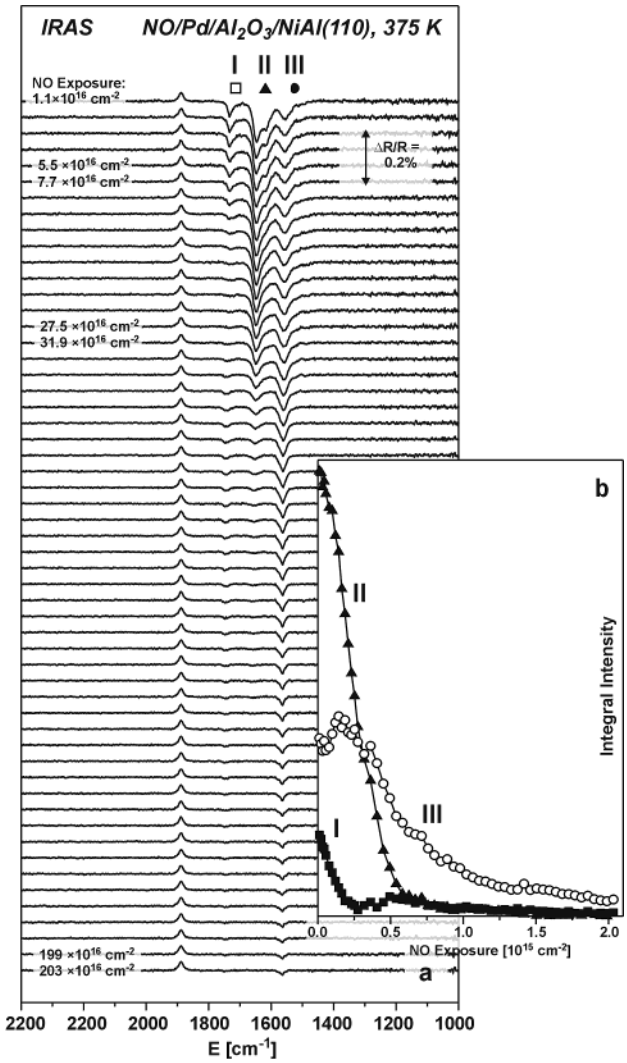

Figure 4. (a) IR spectra of the NO stretching frequency region for the Pd/alumina model catalyst during exposure to a molecular beam of NO at a sample temperature of 375 K; (b) integral absorption in the spectral region indicated in part a.

In Figure 5, the exposure dependence of the different spectral features is displayed as a function of sample temperature. Similar behavior to that at 375 K is observed at all sample temperatures

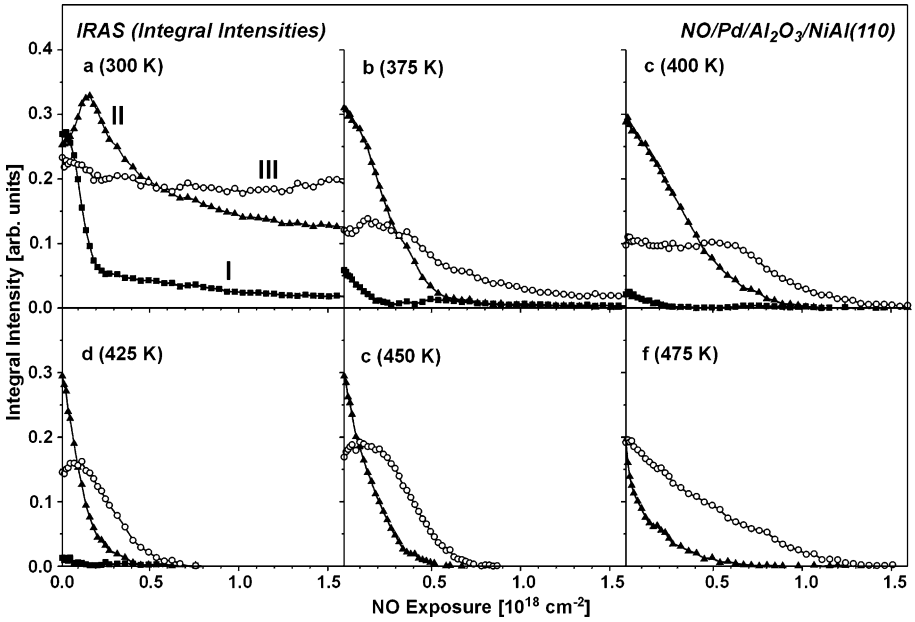

Figure 5. Integral absorption in the different NO stretching frequency regions indicated in Figure 2 as a function of the NO dose and the surface temperature during exposure of the Pd/alumina model catalyst to a molecular beam of NO.

above this value: First, the bands in region (II) are affected before the absorption signal in region (III) starts to decrease at later time. The band in region (I), corresponding to relatively weakly bound on-top NO, cannot be detected anymore at temperatures $T \geq 425$ K. Upon inspection of the low-temperature behavior (300 K), we again find a decreasing intensity in regions (I) and (II) with increasing NO dose. In contrast to this, the intensity of band (III) remains unaffected, even at the highest NO doses. Thus, it becomes clear that the constant total absorption intensity observed at 300 K in the high-coverage limit is mainly due to the bands in region (III).

Following the assignment given in section 3.2, we conclude from these results that the atomic dissociation products of NO preferentially occupy the particle edge and defect sites that are responsible for absorption in regions (I) and (II). A similar observation was made in an STM study of oxygen adsorption on the same Pd model catalyst, showing preferential adsorption at particle edges.[48] Also, atomic carbon was recently shown to exhibit a preference for adsorption at the particle edge and defect sites.[11]

We may invoke two mechanisms that could lead to the fact that nitrogen and oxygen atoms are mainly located in the vicinity of particle edges and steps: (1) First, the NO dissociation could preferentially occur at or in the vicinity of edge or step sites, and diffusion of the reaction products onto the facets could be suppressed. (2) Second, the step and edge sites may represent energetically preferred chemisorption sites so that, irrespective of the actual dissociation site, the products could diffuse to the edges where they would be preferentially adsorbed.

If we first consider the regime of elevated temperatures ($T \geq 375$ K), then we find that the particles eventually lose their full absorption capacity (i.e., diffusion of atomic adsorbates onto the particle facets must be possible). The fact that preferential occupation of particle edge sites is observed over the full temperature range up to 475 K suggests that there is indeed an energetic preference for edge and step sites. Currently, theoretical calculations are being performed to verify this effect for different types of adsorbates.

For low surface temperatures (300 K), the situation is different. Here, the fact that only the particle edge and step features (regions (I) and (II)) are modified by the dissociation products and the reaction stops before the facet peak (region (III)) is affected strongly indicates (a) that dissociation indeed occurs at or in the vicinity of the particle steps or edges (and possibly on the small fraction of (100) facets as well) and (b) that the limited mobility of adsorbates prevents diffusion onto the (111) facets.

To verify this hypothesis, we analyze in detail the changes in the IR spectra that occur upon NO dissociation. Some representative spectra are displayed in Figure 6. At elevated sample temperature ($T \geq 375$ K), we observe a pronounced blue shift for the bands in all three NO stretching frequency regions. At 375 K, for example, the bands shift from initial values of 1733 cm^{-1} (region (I)), 1646 cm^{-1} (region (II)), and 1554 cm^{-1} (region (III)) to 1746 cm^{-1} (region (I)), 1655 cm^{-1} (region (II)), and 1564 cm^{-1} (region (III)), respectively, after exposure to 1.2×10^{18} NO molecules·cm^{-2}.

We interpret these observations on the basis of previous coadsorption studies in which we have investigated the influence of oxygen on the IR spectra of NO on the Pd model catalyst.[29] Typically, pronounced blue shifts of up to 30 cm^{-1} were found for all spectral features. Similar effects were observed for NO and O coadsorption on Pd single-crystal surfaces[49] as well as on other transition metals.[50] Typically, the blue shift is interpreted in terms of a strengthening of the N−O bond due to the electronegative oxygen coadsorbate, reducing the NO $2\pi^*$ electron density. Following this argument, we would expect coadsorbed nitrogen to have a qualitatively similar but possibly less pronounced effect on the NO spectra. Consequently, we can attribute the blue shift observed in the spectra in Figure 6b and c to the presence of coadsorbed atomic nitrogen and oxygen in the vicinity of the corresponding NO species. Because similar shifts are observed for the entire spectral region, this implies that at 375 K and above the atomic reaction products are present both at the edges and steps of the particles and on the facets.

At low sample temperature (300 K), the situation is entirely different (Figure 6a). Whereas the bands in regions (I) and (II) are subject to a pronounced blue shift from 1734 (region (I)) and 1655 cm^{-1} (region (II)) to 1750 and 1670 cm^{-1}, respectively (at an exposure of 1.6×10^{18} NO molecules·cm^{-2}), the band

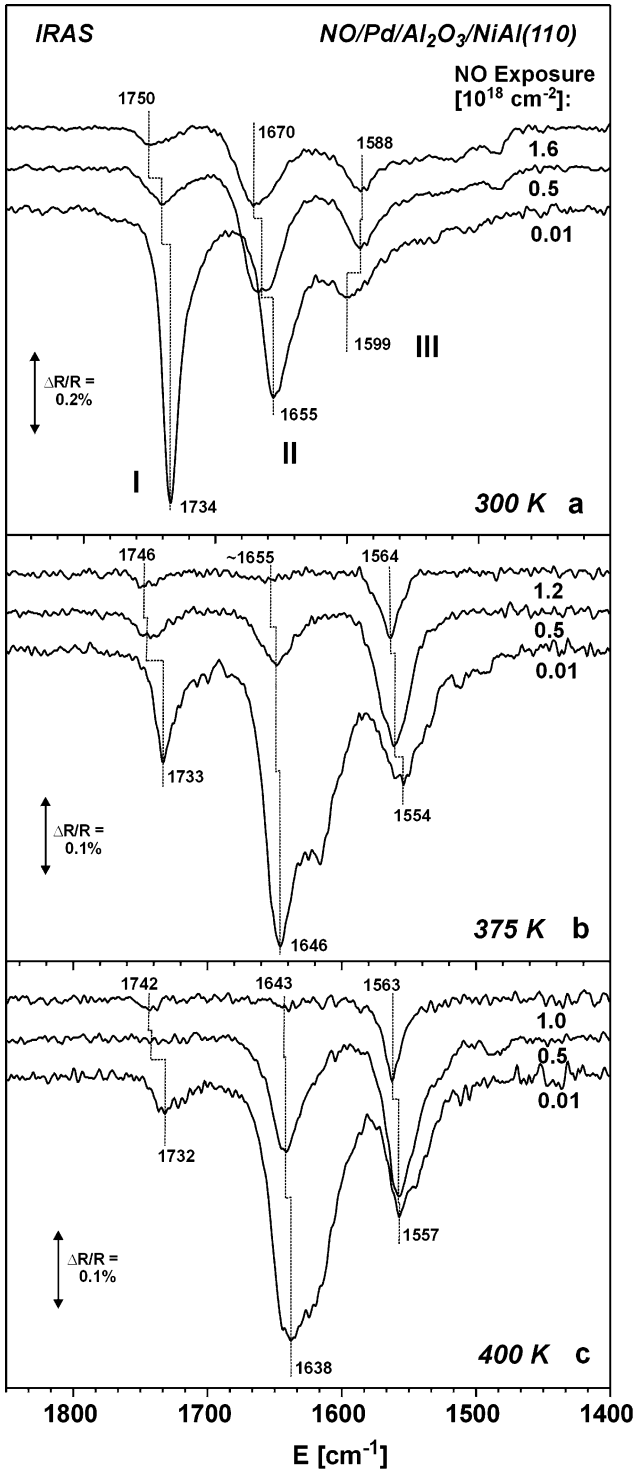

Figure 6. Selected IR spectra of the NO stretching frequency region at different surface temperatures and NO doses recorded during exposure of the Pd/alumina model catalyst to a molecular beam of NO.

in region (III) exhibits a shift in the reverse direction (i.e., a red shift from 1599 to 1588 cm^{-1}). This observation suggests the absence of atomic nitrogen or oxygen on the particle facets, which is in line with the previous hypothesis, assuming the diffusion of the atomic species from the reactive sites onto the (111) facets to be suppressed at 300 K. The shift to lower frequency might indicate a change in the structure and density of the adsorbate layer (e.g., that due to a modified adsorbate−adsorbate interaction at the particle edges), which become depleted of NO during the experiment.

The hypothesis that only a few specific sites are responsible for the dissociation activity appears to be natural for the supported Pd particles because it is well established that NO dissociation exhibits a pronounced structure dependency on Pd single-crystal surfaces. Whereas on Pd(111) NO remains intact up to high temperatures, Pd(100) and stepped Pd surfaces exhibit much higher activity toward dissociation. (See, for example, refs 20−23, and 25 and references therein.) These differences in activity have been confirmed by theoretical calculations as well.[51,52] Consequently, large differences in activity are also expected for different sites on a supported particle, giving rise to structure and size effects that have indeed been observed experimentally.[26,27]

Concerning the NO dissociation kinetics, it is worth noting that the nitrogen and oxygen accumulation rate goes through a maximum around 425 K. As possible reasons for the decreasing rate of product accumulation at higher temperature, we may assume that the population of reactive sites decreases, resulting in an overall decrease in the dissociation rate. As a second factor, we may invoke the formation of N_2O, which may lead to the partial removal of adsorbed nitrogen at sufficiently high sample temperatures.[23,25] An exact quantification of the occupation of different sites is difficult to make on the basis of IRAS experiments; therefore, the microscopic origin of this subtle kinetic effect cannot yet be elucidated on the basis of the present experiments.

As an important inference, the above results imply that the onset temperature at which the atomic reaction products become mobile under reaction conditions on the time scale of the experiment (5×10^3 s) and on the length scale of the particles (6 nm) lies in the range between 300 and 375 K. In a simple estimate based on the Einstein relation and a diffusion coefficient with a normal prefactor (10^{-3} $cm^2 \cdot s^{-1}$), this would correspond to a diffusion barrier in the range of 0.7 to 0.9 eV. Unfortunately, the amount of experimental data on oxygen and nitrogen diffusion on Pd surfaces is limited. For oxygen diffusion, we have recently estimated an upper limit of 0.85 eV [53] for the diffusion barrier on the Pd particles under conditions of the CO oxidation reaction. Recent theoretical calculations for O diffusion on Pd(111) yielded a barrier of 0.54 eV.[54] More detailed data is available on other transition-metal surfaces such as Ru(0001), where the diffusion barriers for N and O were calculated as 0.79 and 0.54 eV, respectively.[55] Experimentally, the diffusion barrier for N on Ru(0001) was determined to be 0.94 eV.[56] We have to keep in mind, however, that the latter experimental and theoretical results typically correspond to the low-coverage limit. In the current experiments, however, diffusion is probed under conditions of high adsorbate coverage and, in particular, under conditions of high steady-state NO coverage. This coadsorbed NO may lead to a reduced diffusion of the atomic adsorbates. On the basis of these considerations, it appears plausible that the mobility of not only nitrogen atoms but also oxygen atoms is suppressed at low reaction temperature (300 K), as suggested by the experimental data discussed above.

3.4. Site Occupation Studied Using CO as a Probe Molecule. To verify further the results and assignments of the adsorption sites given in the previous section, we have performed additional experiments using CO as a probe molecule. The spectroscopic assignment of the IR spectra of adsorbed CO on the supported Pd model catalyst, serving as a basis for these experiments, has been discussed recently[46] (Table 1). Detailed descriptions of related studies can be found elsewhere.[11,57,58]

Briefly, the CO stretching frequency region is investigated after CO saturation at 300 K (IR spectra taken at 100 K). Three

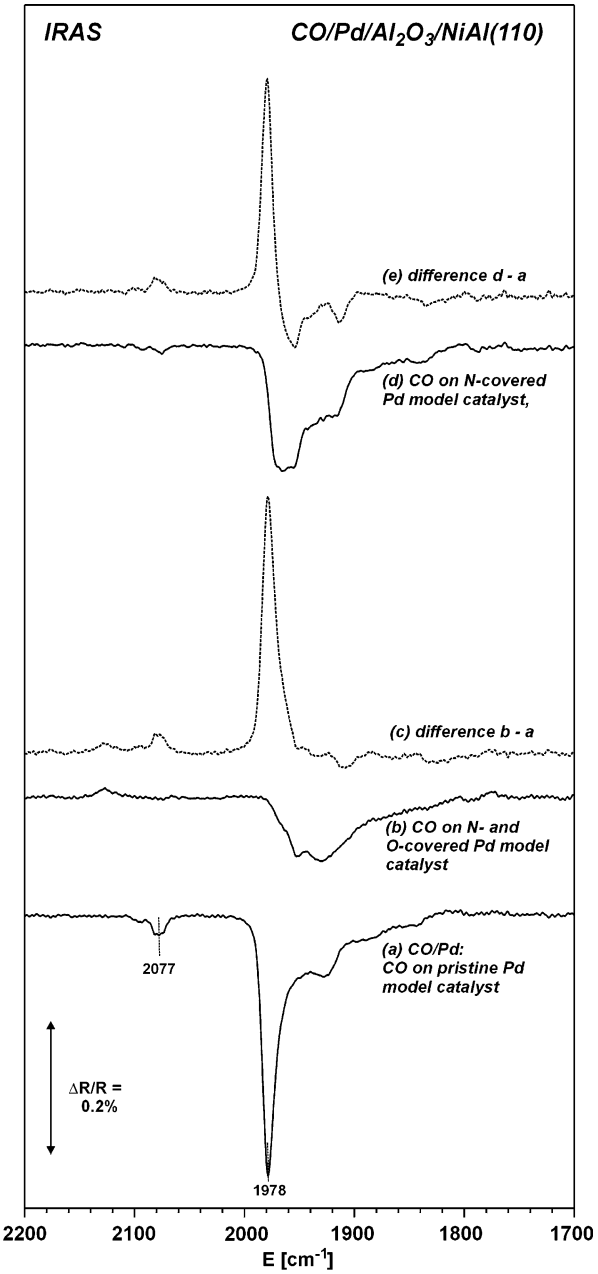

Figure 7. IR spectra of the CO stretching frequency region recorded at a surface temperature of 100 K: (a) after CO saturation of the pristine Pd model catalyst at 300 K; (b) for the oxygen and nitrogen precovered particles prepared by prolonged exposure to NO at 430 K and subsequent CO saturation at 300 K; (c) difference between a and b; (d) for nitrogen precovered particles preperared by prolonged exposure to NO at 430 K, subsequent CO exposure at 420 K (to remove surface oxygen), and finally CO saturation at 300 K; (e) difference between a and d (see the text for details).

principal spectral regions are identified for the pristine sample (Figure 7a). The spectrum is dominated by a sharp absorption band at 1978 cm^{-1} with a series of weaker low-frequency features (down to 1840 cm^{-1}) and an additional weak band at 2077 cm^{-1}. Previously, the low-frequency features were assigned to CO adsorbed mainly on hollow sites on Pd(111) facets, and the absorption peak around 2077 cm^{-1} was assigned to on-top CO, partially on defect sites. A comparison with previous work and theoretical calculations shows that the prominent absorption band around 1970 cm^{-1} originates from a superposition of bridge-bonded CO on (100) facets and CO adsorbed at defect sites such as particle edges or steps.[46] For reasons similar to those discussed in connection with the NO spectra (section 3.2), the edge and step contribution is expected to dominate. Again, it should be noted that the relative intensities do not reflect the relative abundance of the corresponding sites.

Following this assignment, we can use the CO as a probe for the occupation of particle sites by strongly bound atomic species. For this purpose, we prepare a partially nitrogen- and oxygen-covered surface by NO exposure at 440 K. Subsequently, the surface is CO saturated, and a spectrum is recorded following the same experimental procedure as for the pristine sample. The corresponding IR spectra and the difference with respect to the clean Pd model catalyst surface are displayed in Figure 7a−c, respectively. In a last step, the oxygen was selectively removed from the surface by applying a pulse of CO at elevated sample temperature (430 K). Finally, an IR spectrum of the CO-saturated particles partially precovered by pure nitrogen was recorded according to the procedure given above. Again, the corresponding spectrum of the CO stretching frequency region and the difference with respect to the clean model catalyst is displayed in Figure 7d and e.

We observe that in all cases only weak changes occur in the spectral region assigned to the particle (111) facets. The slight increase in intensity here, especially for the nitrogen-covered sample, can be attributed to a weaker intensity transfer to the higher-frequency band due to the reduced dipole coupling. In contrast to the low-frequency region, the strong attenuation of the band around 1970 cm^{-1} indicates a strong loss of bridge-bonded CO from the particle edges, steps, or defects. This effect is the most pronounced for the nitrogen and oxygen precovered particles but is still rather strong for the purely nitrogen-covered situation. In line with the results obtained from the IR spectra of NO adsorption, this behavior indicates that the adsorption of both nitrogen and oxygen preferentially occurs at the particle edges and defects, leading to a modification of the adsorption properties of these sites. Thus, IR spectroscopy of adsorbed CO can be employed as a site-sensitive probe, as an alternative to the direct spectroscopic approach used in section 3.3. Finally, it is noteworthy that in the CO case some chemical specifity regarding the nature of the coadsorbed species arises from the fact that not all of the adsorption sites are affected in a similar manner by all coadsorbates. For example, it was found in a previous study that carbon coadsorption results in a strong population of on-top sites by CO (around 2080 cm^{-1}) under the experimental conditions applied here,[46] whereas the nitrogen and oxygen coadsorbates apparently do not show this effect. Possible explanations for these dissimilarities include differences in the effect of the coadsorbate on the electronic structure of the surrounding metal atoms and also the occupation of different particle edge sites and different affinities of the atomic adsorbates to form subsurface species.[59]

3.5. Relation between Site Occupation and NO Dissociation Kinetics. The experimental procedures, which allow us to monitor and manipulate the occupation of specific sites on the supported Pd particles, also open up the possibility to investigate the influence of specific coadsorbates on the catalytic activity of these sites. A corresponding experiment is briefly illustrated in Figure 8. A more detailed description can be found elsewhere.[60,61] First, the dissociation of NO is followed by means of IR spectroscopy in an experiment identical to those displayed in Figure 5. As described before, the fact that the high-frequency band in region (II) vanishes first and the band in region (III) vanishes at a later time indicates the preferential adsorption of atomic nitrogen and oxygen in the vicinity of edge and step sites on the Pd particles. Finally, the particles become fully

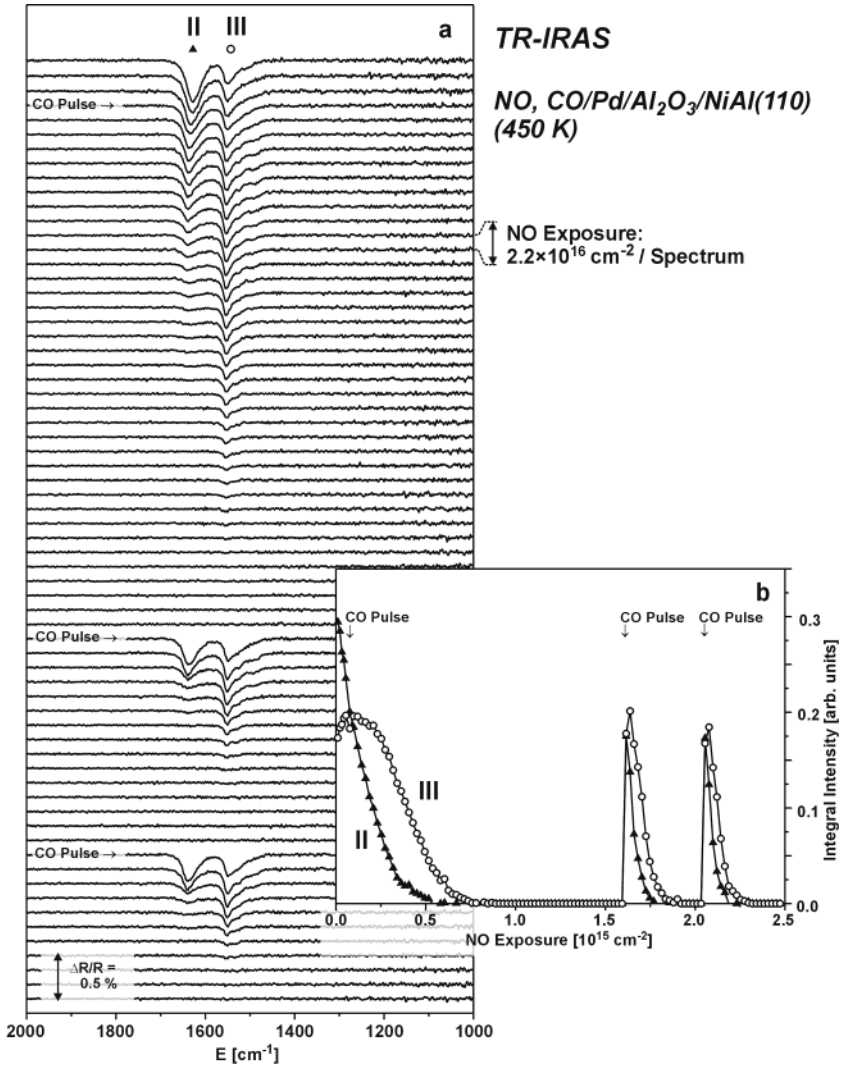

Figure 8. (a) IR spectra of the NO stretching frequency region for the Pd/alumina model catalyst during exposure to a molecular beam of NO at a sample temperature of 450 K. At the times indicated, a pulse of CO was applied via a second molecular beam source to remove surface oxygen selectively from the Pd particles; (b) integral absorption in the spectral region indicated in part a.

covered by the atomic dissociation products, leading to a complete loss of the NO adsorption capacity.

As already indicated in section 3.4, adsorbed atomic oxygen can be efficiently removed from the particles by exposing the sample to CO. The CO_2 produced desorbs from the surface instantaneously. Thus, we may apply a strong pulse of CO at arbitrary time to remove adsorbed oxygen selectively in a process that is fast on the time scale of the NO dissociation experiment. This procedure allows us to differentiate between the effect of adsorbed atomic oxygen and nitrogen on the dissociation activity.

A corresponding experiment is displayed in Figure 8. The first CO pulse is applied shortly after opening the NO beam. As expected for the low oxygen coverage at this point, there is no pronounced effect on the spectra or the kinetics. A second CO pulse is applied after the particles have completely lost their NO adsorption capacity because of oxygen and nitrogen accumulation. Substantial CO_2 production as monitored by quadrupole mass spectrometry indicates a large oxygen coverage at this point. After the removal of the surface oxygen, the band assigned to NO on Pd facets (III) is fully restored, whereas the absorption band assigned to NO at particle edges and steps (II) is only partially restored and remains blue-shifted. In line with the discussion in section 3.3, we can conclude from this observation that a sufficiently strongly bound nitrogen species remains adsorbed on the particles and is located preferentially in the vicinity of edge and step sites. Similar strongly adsorbed nitrogen species have been observed both on Pd single-crystal surfaces and on supported particles.[24,25] It should be noted that the CO titration experiment can be repeated several times without any significant decrease in the NO band intensity or CO_2 yield, implying that there is no change in the NO dissociation capacity and, consequently, no further accumulation of nitrogen beyond the amount formed initially. This means that a well-defined part of the surface nitrogen leaves the surface via the formation of N_2 or N_2O. The formation of these products has been proven experimentally in studies on different Pd single crystals.[23,25]

The most surprising observation, however, is the fact that after initial oxygen removal the rate at which the surface is covered by the reaction products becomes much faster. As mentioned before, CO titration experiments show that this effect is not due to a loss in the adsorption capacity. Therefore, the NO dissociation rate must be significantly enhanced on the purely nitrogen-covered surface.

There are two important points that follow from this observation. First, we conclude that the "irregular" sites on the particles such as edges, steps, or defects dominate the dissociation activity. This is in line with the results discussed in connection with the temperature dependence of the dissociation behavior

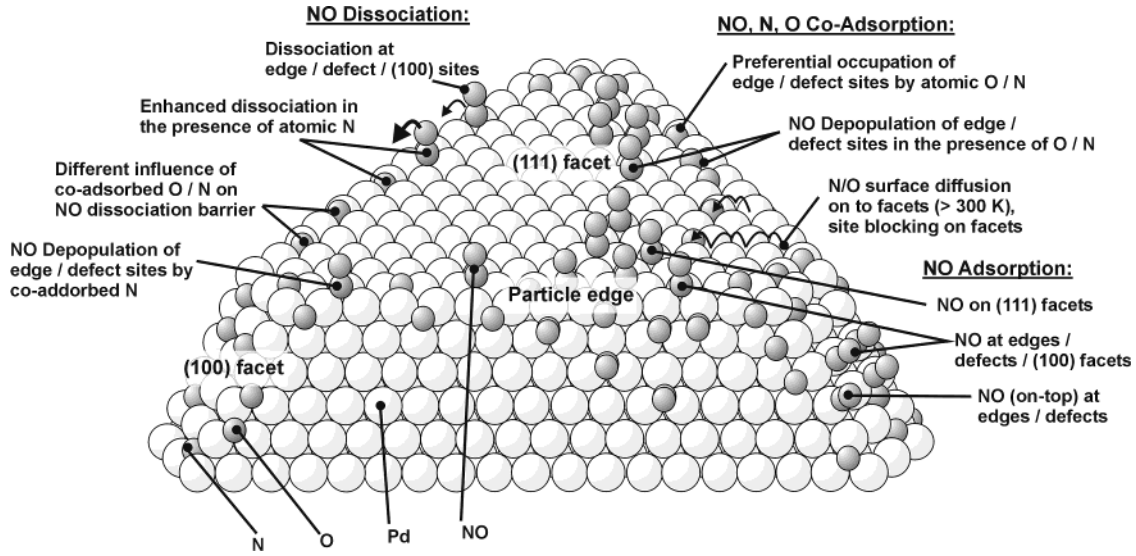

Figure 9. Schematic representation of the adsorption, surface diffusion, and reaction processes studied in this work.

and the commonly accepted strong structure dependence of the NO dissociation step. (See the discussion in section 3.3). The second and less well established point is that the results clearly demonstrate that the atomic coadsorbate species bound in the vicinity of the particle edges critically control the dissociation activity. Thus, a detailed understanding of the behavior and effect of these species is crucial in a microscopic description of the kinetics of the NO dissociation and reduction.

Previously, we considered two effects that might contribute to the increased dissociation rate. First, the presence of strongly bound nitrogen may give rise to a partial depopulation of the active sites with respect to NO, leading to a reduced site-blocking effect. Second, it is likely that nitrogen and oxygen species coadsorbed in the vicinity of the active metal site have different effects on its electronic structure and, therefore, on the activation barrier for NO dissociation. Thus, a possible scenario would imply different decorations of the active sites by oxygen and nitrogen. Currently, theoretical calculations are in progress that may help to identify the exact mechanism.

4. Conclusions

In conclusion, we have investigated the role of different adsorption and reaction sites on a structurally well-defined Pd/alumina model catalyst. The supported Pd particles have been characterized in detail previously. They have an average diameter of approximately 5.5 nm (3000 Pd atoms) and are mainly terminated by (111) facets and a small fraction of (100) facets. We employ a combination of in-situ TR-IRAS and molecular beam methods to obtain spectroscopic and kinetic information about the NO adsorption, surface diffusion, and dissociation on these particles under exactly controlled reaction conditions.

During the interaction with NO, several processes are investigated; these are summarized in the schematic representation in Figure 9:

- As a first step, the IR spectra of NO on the supported Pd particles are investigated as a function of surface temperature. Several spectral regions are identified and assigned to (I) NO adsorbed at on-top sites at particle edges, steps, and defects, (II) NO most likely adsorbed in a bridging configuration at particle edges, steps, and defects, and (III) NO adsorbed at hollow sites on (111) facets.
- Second, the kinetics of NO dissociation and the effect of the coadsorbed dissociation products, atomic nitrogen and oxygen, on the vibrational spectra of NO are investigated for the reaction conditions: (1) It is found that the coadsorbed atomic dissociation products give rise to a pronounced blue shift of nearby NO species. (2) It is concluded that NO dissociation occurs on the Pd particles at temperatures $T \geq 300$ K. (3) The dissociation activity is found to be dominated by particle edges, steps, defects, and (100) sites rather than by the majority of (111) facets. (4) Under the reaction conditions, the surface diffusion of atomic oxygen and nitrogen is suppressed at temperatures up to 300 K. At higher temperature, the atomic products can migrate onto the particle facets. (5) Atomic nitrogen and oxygen species are found to adsorb preferentially at sites in the vicinity of particle edges and defects over the full temperature range studied.
- Using CO as a probe molecule, we verified the preferential occupation of particle edges and defect sites by atomic nitrogen and oxygen.
- Finally, the influence of atomic nitrogen and oxygen on the kinetics of NO dissociation is probed. It is observed that under the reaction conditions employed in this study (relatively low temperature and high adsorbate coverage) the atomic adsorbates in the vicinity of particle edges and defects have a significant influence on the reaction rate. Specifically, it is shown that in the presence of strongly bound atomic nitrogen the NO dissociation probability is drastically enhanced.

Acknowledgment. We acknowledge the financial support of this project by the Volkswagen Foundation (Program of Partnerships, "The Mechanism and Kinetics of NO Reduction Reactions on Noble Metal Surfaces − From Single Crystal Surfaces to Supported Model Catalysts").

References and Notes

(1) Ertl, G., Knoezinger, H., Weitkamp, J., Eds. *Handbook of Heterogeneous Catalysis*; VCH: Weinheim, Germany, 1997.
(2) Freund, H.-J.; Libuda, J.; Bäumer, M.; Risse, T.; Carlsson, A. *Chem. Rec. Age* **2003**, *3*, 181.
(3) Henry, C. R. *Surf. Sci. Rep.* **1998**, *31*, 231.
(4) Zhdanov, V. P.; Kasemo, B. *Surf. Sci. Rep.* **2000**, *39*, 25.
(5) St. Clair, T. P.; Goodman, D. W. *Top. Catal.* **2000**, *13*, 5.
(6) Jaeger, R. M.; Kuhlenbeck, H.; Freund, H.-J.; Wuttig, M.; Hoffmann, W.; Franchy, R.; Ibach, H. *Surf. Sci.* **1991**, *259*, 235.
(7) Libuda, J.; Winkelmann, F.; Bäumer, M.; Freund, H.-J.; Bertrams, T.; Neddermeyer, H.; Müller, K. *Surf. Sci.* **1994**, *318*, 61.
(8) Bäumer, M.; Freund, H.-J. *Prog. Surf. Sci.* **1999**, *61*, 127.
(9) Libuda, J.; Freund, H.-J. *J. Phys. Chem. B* **2002**, *106*, 4901.

(10) Meusel, I.; Hoffmann, J.; Hartmann, J.; Libuda, J.; Freund, H.-J. *J. Phys. Chem. B* **2001**, *105*, 3567.
(11) Schauermann, S.; Hoffmann, J.; Johánek, V.; Hartmann, J.; Libuda, J.; Freund, H.-J. *Angew. Chem., Int. Ed.* **2002**, *41*, 2513.
(12) Hoffmann, J.; Schauermann, S.; Johánek, V.; Hartmann, J.; Libuda, J. *J. Catal.* **2003**, *213*, 176.
(13) Kreuzer, T.; Lox, S. E.; Lindner, D.; Leyrer, J. *Catal. Today* **1996**, *29*, 17.
(14) Salasc, S.; Skoglundh, M.; Fridell, E. *Appl. Catal., B* **2002**, *36*, 145.
(15) Holles, J. H.; Davis, R. J.; Murray, T. M.; Howe, J. M. *J. Catal.* **2000**, *195*, 193.
(16) Martinez-Arias, A.; Fernandez-Garcia, M.; Hungria, A. B.; Iglesias-Juez, A.; Duncan, K.; Smith, R.; Anderson, J. A.; Conesa, J. C.; Soria, J. *J. Catal.* **2001**, *204*, 238.
(17) Zhdanov, V. P.; Kasemo, B. *Surf. Sci. Rep.* **1997**, *29*, 31.
(18) Gopinath, C. S.; Zaera, F. *J. Catal.* **2001**, *200*, 270.
(19) Gopinath, C. S.; Zaera, F. *J. Phys. Chem. B* **2000**, *104*, 3194.
(20) Ramsier, R. D.; Gao, Q.; Neergaard Waltenburg, H.; Lee, K.-W.; Nooij, O. W.; Lefferts, L.; Yates, J. T., Jr. *Surf. Sci.* **1994**, *320*, 209.
(21) Ramsier, R. D.; Gao, Q.; Neergaard Waltenburg, H.; Yates, J. T., Jr. *J. Chem. Phys.* **1994**, *100*, 6837.
(22) Sugai, S.; Watanabe, H.; Kioka, T.; Miki, H.; Kawasaki, K. *Surf. Sci.* **1991**, *259*, 109.
(23) Sharpe, R. G.; Bowker, M. *Surf. Sci.* **1996**, *360*, 21.
(24) Rainer, D. R.; Vesecky, S. M.; Koranne, M.; Oh, W. S.; Goodman, D. W. *J. Catal.* **1997**, *167*, 234.
(25) Hirsimaki, M.; Valden, M. *J. Chem. Phys.* **2001**, *114*, 2345.
(26) Piccolo, L.; Henry, C. R. *Appl. Surf. Sci.* **2000**, *162*−*163*, 670.
(27) Prevot, G.; Henry, C. R. *J. Phys. Chem. B* **2002**, *106*, 12191.
(28) Schauermann, S.; Johánek, V.; Laurin, M.; Libuda, J.; Freund, H.-J. *Chem. Phys. Lett.* **2003**, *381*, 298.
(29) Schauermann, S.; Johánek, V.; Laurin, M.; Libuda, J.; Freund, H.-J. *Phys. Chem. Chem. Phys.* **2004**, *6*, 5139.
(30) Libuda, J.; Meusel, I.; Hartmann, J.; Freund, H.-J. *Rev. Sci. Instrum.* **2000**, *71*, 4395.
(31) Meusel, I.; Hoffmann, J.; Hartmann, J.; Heemeier, M.; Bäumer, M.; Libuda, J.; Freund, H.-J. *Catal. Lett.* **2001**, *71*, 5.
(32) Shaikhutdinov, S.; Heemeier, M.; Hoffmann, J.; Meusel, I.; Richter, B.; Bäumer, M.; Kuhlenbeck, H.; Libuda, J.; Freund, H.-J.; Oldman, R.; Jackson, S. D.; Konvicka, C.; Schmid, M.; Varga, P. *Surf. Sci.* **2002**, *501*, 270.
(33) Bertolo, M.; Jacobi, K.; Nettesheim, S.; Wolf, M.; Hasselbrink, E. *Vacuum* **1990**, 76.
(34) Bertolo, M.; Jacobi, K. *Surf. Sci.* **1990**, *226*, 207.
(35) Conrad, H.; Ertl, G.; Küppers, J.; Latta, E. E. *Surf. Sci.* **1977**, *65*, 235.
(36) Wickham, D. T.; Banse, B. A.; Koel, B. E. *Surf. Sci.* **1991**, *243*, 83.
(37) Chen, P. J.; Goodman, D. W. *Surf. Sci.* **1993**, *297*, L93.
(38) Loffreda, D.; Simon, D.; Sautet, P. *Chem. Phys. Lett.* **1998**, *291*, 15.
(39) Loffreda, D.; Simon, D.; Sautet, P. *J. Chem. Phys.* **1998**, *108*, 6447.
(40) Honkala, K.; Pirilä, P.; Laasonen, K. *Surf. Sci.* **2001**, *489*, 72.
(41) Brown, W. S.; King, D. A. *J. Phys. Chem. B* **2000**, *104*, 2578.
(42) Nyberg, C.; Uvdal, P. *Surf. Sci.* **1988**, *204*, 517.
(43) Jaworowski, A. J.; Asmundsson, R.; Uvdal, P.; Sandell, A. *Surf. Sci.* **2002**, *501*, 74.
(44) Nakamura, I.; Fujitani, T.; Hamada, H. *Surf. Sci.* **2002**, *514*, 409.
(45) Hoffmann, F. M. *Surf. Sci. Rep.* **1983**, *3*, 107.
(46) Yudanov, I. V.; Sahnoun, R.; Neyman, K. M.; Rösch, N.; Hoffmann, J.; Schauermann, S.; Johánek, V.; Unterhalt, H.; Rupprechter, G.; Libuda, J.; Freund, H.-J. *J. Phys. Chem. B* **2003**, *107*, 255.
(47) Hollins, P. *Surf. Sci. Rep.* **1992**, *16*, 51.
(48) Hansen, K. H.; Sljivancanin, Z.; Laegsgaard, E.; Besenbacher, F.; Stensgaard, I. *Surf. Sci.* **2002**, *505*, 25.
(49) Nyberg, C.; Uvdal, P. *Surf. Sci.* **1991**, *256*, 42.
(50) Chen, J. G.; Erley, W.; Ibach, H. *Vacuum* **1990**, *41*, 74.
(51) Hammer, B. *J. Catal.* **2001**, *199*, 171.
(52) Hammer, B. *Phys. Rev. Lett.* **2002**, *89*, 016102.
(53) Hoffmann, J.; Schauermann, S.; Hartmann, J.; Zhdanov, V. P.; Kasemo, B.; Libuda, J.; Freund, H.-J. *Chem. Phys. Lett.* **2002**, *354*, 403.
(54) Honkala, K.; Laasonen, K. *J. Chem. Phys.* **2001**, *115*, 2297.
(55) Hammer, B. *Surf. Sci.* **2000**, *459*, 323.
(56) Zambelli, T.; Trost, J.; Wintterlin, J.; Ertl, G. *Phys. Rev. Lett.* **1996**, *76*, 795.
(57) Schauermann, S.; Hoffmann, J.; Johánek, V.; Hartmann, J.; Libuda, J.; Freund, H.-J. *Catal. Lett.* **2002**, *84*, 209.
(58) Bertarione, S.; Scarano, D.; Zecchina, A.; Johanek, V.; Hoffmann, J.; Schauermann, S.; Frank, M.; Libuda, J.; Rupprechter, G.; Freund, H.-J. *J. Phys. Chem. B* **2004**, *108*, 3603.
(59) Yudanov, I. V.; Neyman, K. M.; Rösch, N. *Phys. Chem. Chem. Phys.* **2004**, *6*, 116.
(60) Johanek, V.; Schauermann, S.; Laurin, M.; Libuda, J.; Freund, H.-J. *Angew. Chem., Int. Ed.* **2003**, *42*, 3035.
(61) Frank, M.; Bäumer, M. *Phys. Chem. Chem. Phys.* **2000**, *2*, 3723.